

Damage Curve Approach in Fatigue Using Acoustic Emission Technique

R. VISWESWARAN*, R. KRISHNAKUMAR**,
M. R. PRANESH*** and O. PRABHAKAR†

**American Bureau of Shipping, Madras, India*

***Senior Project Officer, CAD/CAM Programme; ***Principal Scientific Officer, Ocean Engineering Centre; †Professor, Department of Metallurgical Engineering; The Indian Institute of Technology, Madras, India*

ABSTRACT

Progressive fatigue damage has been assessed in tensile-tensile mode ($R=0.1$) using acoustic emission technique. The experiments were conducted in laboratory environment using low carbon steels (IS 2062, AISI 1008), a material used often in offshore structures. The nature of the non-linearity of the fatigue damage suffered by the material is discussed with an Acoustic Emission (AE) parameter Ring Down Count. Three active AE stages were found with relatively quiet intervening periods. However, at very high stress ranges, in excess of 33.8 Kg/sq.mm, the stages could not be identified very clearly. This paper also presents a two step (two stress levels) and three step fatigue loading carried out to compare the proposed linear damage law based on AE experiments with the Miner's Damage Rule.

KEYWORDS

Acoustic Emission; fatigue damage; damage accumulation; life prediction.

INTRODUCTION

Assessment of fatigue damage under variable amplitude loading has been an active area of research over the past two decades. It has been hampered by lack of detailed understanding of the physical changes that take place in the material during the period of fatigue life. Miner (1945) was the first to propose a damage rule which today is popularly known as Linear Damage Rule. It has been well recognized that fatigue damage takes place in stages (Tanaka, 1972; Manson et al., 1981; Miller et al., 1977; Hawarth et al., 1977). Attempts have been made to quantify damage based on input parameters and material constants. Chaboche (1977) proposed the following equation based on effective stress concept:

$$D = 1 - \left(1 - \left(\frac{n}{N} \right)^{1/1+Y} \right)^{1/1+B} \quad (1)$$

where B is a material constant and Y is an exponent that depends on the applied load amplitude.

Physical observation of damage on the surface of the specimen has been carried out by Tanaka (1972) using optical microscopy and X-ray diffraction and by Hawarth et al., (1977) using

holographic techniques. It has been noticed that fatigue damage occurs in three stages consisting of slip band formation, micro-cracking and crack propagation. However, Pangborn et al.,(1981) recognised the need for evaluating the damage taking place in the bulk material and have studied the dislocation density and distribution using X-Ray double crystal diffractometry. Molybdenum K-Alpha radiation has been used to assess damage upto a maximum depth of 400 microns. The above studies do not take into account damage in the bulk of the material but only that which occurs on the surface and in the sub-surface of the material.

Acoustic Emission (AE) is an elastic stress wave emission which can be gathered on a real time basis while the material is actually undergoing damage. This technique lends itself to relatively easy condition monitoring of any equipment or structure under load. AE technique has the advantage, particularly useful in ocean structures, of being able to assess fatigue damage prior to initiation of cracks. It can be correlated to micro-plastic strain occurring in the entire material (Harris et al.,1984). This paper presents a method of using AE to quantify the total fatigue damage occurring in the material. Fatigue experiments were carried out on low carbon steel material at different stress amplitudes. The AE output was recorded and an attempt was made to characterize the fatigue damage through the AE parameter Ring Down Count (RDC).

EXPERIMENTAL PROCEDURE

The chemical composition and the mechanical properties of the low carbon steel specimen material are given in Table 1.

Table 1: Chemical composition of the steel used (percentage).

C	Mn	P	S	Si	Cu	Cr	Ni	Al
0.08	0.53	0.015	0.022	0.06	traces	0.02	traces	0.1

Mechanical Properties: Ultimate Tensile Strength ; 41.0 Kg/sq.mm;
Yield Strength :32.8 Kg/sq.mm; Elongation : 22.8%.

A flat specimen 3.0 mm thick and a minimum width of 20 mm was used. The dimensional details of the specimens used are shown in Fig.1b. Before fatigue testing, the test specimens were normalised at 900 C and specimen surfaces were subsequently ground using fine surface grinding wheel. Fatigue testing was carried out using a MTS 810 Material Testing System which is a general purpose closed loop electro hydraulic servo controlled system designed to carry out static and dynamic testing. In the present set of experiments, a nylon disc was introduced in the top portion between the loading flange and grip assembly and a bakelite disc was introduced in the lower part of the loading frame to reduce the grip noise to a minimum. A micro processor based AE monitoring system consisting of AET 5000 CPU , Advantage terminal, AET 375 KHz sensors, AET preamplifiers and 250-500 KHz filters were used to collect the AE signals emitted by the specimen during fatigue testing. The system software permits AE signal discrimination based on any or all signal parameters. Threshold of the signal (to eliminate electronic and background noise) can be set on either fixed or automatic mode. In the present set of experiments, a threshold of 1.5 volts, was maintained in the automatic mode. This was 5 times the basic noise level of 300 millivolts. Figure 1a shows the schematic layout of test set-up employed for testing tensile-fatigue specimens.

Tensile Fatigue Tests

Fatigue tests were conducted in laboratory environment under tension/tension load (sine wave) having R value (Minimum stress/Maximum stress) of 0.1. The stress ranges employed in the present fatigue testing are given in Table 2.

Acoustic Emission Data : Fatigue Testing

Event rate and ring down count (RDC) rate recorded as a function of time during fatigue testing are shown in Figs. 2 and 3 . The RDC and Events were aggregated over time spans of 240 seconds and 120 seconds respectively. These two represent two typical curves obtained in this set of experiments. In addition, Fig. 4 shows the cumulative values of RDC plotted as a function of cycles.

Figure 5 schematically represents the different stages in fatigue life (Ewalds et al.,1985). Though these stages are fundamental to fatigue phenomenon the time at which they take place are different for different stress ranges. Number of cycles at the end of fatigue stages as indicated by the AE curves for eleven test specimens are given in Table 2 . The cumulative RDC at the same fatigue stages are also given in Table 2.

Table 2: Number of cycles and cumulative RDC at fatigue stages for varying stress values

Sp. No.	Stress range (Kg/sq.mm)	NUMBER OF CYCLES			CUMULATIVE RDC		
		Stage I Ns	Stage II Nc	Stage III Nf	Stage I	Stage II	Stage III
A	28.7	39 800	290 700	1 638 100	126 000	1 750 000	3 990 000
B	29.2	21 600	210 600	840 600	180 000	660 000	2 730 000
C	29.3	44 800	268 700	639 720	147 500	505 000	690 000
D	29.5	18 840	282 600	753 600	150 000	492 000	600 000
E	30.6	12 690	253 600	422 940	23 500	77 800	141 800
F	31.3	10 090	100 910	201 830	32 000	58 000	137 000
G	31.4	10 710	105 500	162 340	12 500	37 200	46 700
H	33.2	13 110	94 600	163 900	25 000	50 000	65 000
I	33.8	-	8 400	113 600	-	46 600	73 000
J	34.0	-	2 600	16 010	-	7 300	14 500
K	34.1	-	2 350	32 720	-	900	3 300

The relationship between Nf, number of cycles to failure and Stress Range σ can be expressed as follows:

$$\log N_f = 41.91 X (\log \sigma)^{-5.08} \quad (2)$$

The number of stress cycles at the first intense acoustic activity, Ns, and the stress range can be related by the following relationship:

$$\log N_s = 37.20 X (\log \sigma)^{-5.48} \quad (3)$$

The number of stress cycles to the second intense acoustic activity, Nc, and the stress range can be related by the following relationship:

$$\log N_c = 29.79 X (\log \sigma)^{-4.41} \quad (4)$$

Therefore the ratios of Ns and Nc to the number of cycles at fracture, Nf, can be obtained from the equations 2,3 and 4 and the same can be expressed as :

$$N_s : N_c : N_f = 0.03 \text{ to } 0.08 : 0.25 \text{ to } 0.75 : 1 \quad (5)$$

Similarly the number of cycles at the end of each fatigue stage could be replaced by the cumulative RDC and a similar set of three equations could be obtained which are given below.

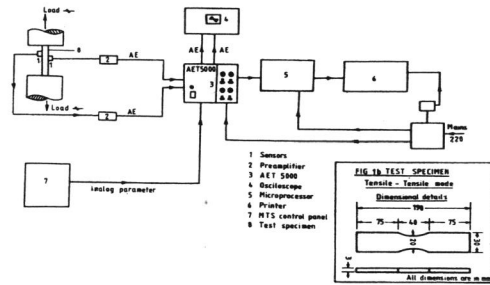


Fig. 1a. Layout of test set up

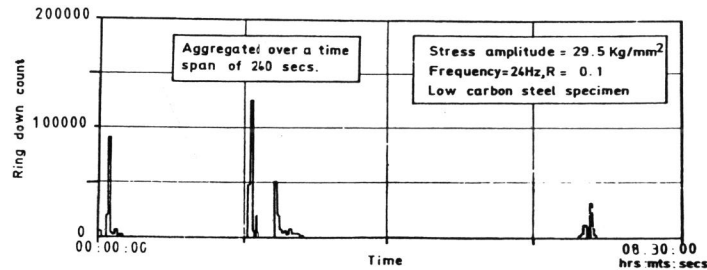


Fig. 2. RDC versus time for specimen D

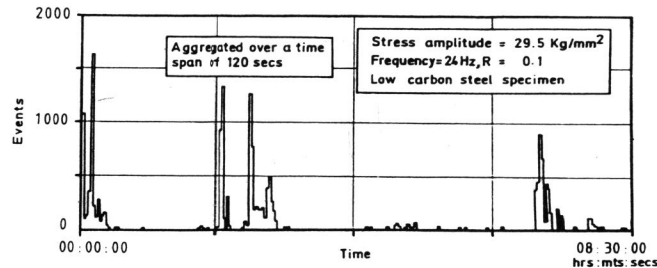


Fig. 3. Events versus time for specimen D

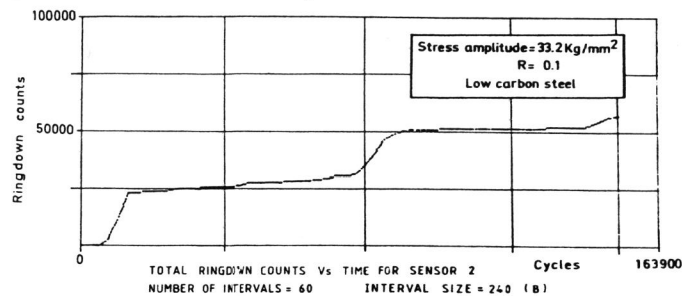


Fig. 4. Cumulative RDC versus cycles

$$\log \text{RDCs} = 56.51 \times (\log \sigma) - 6.32 \quad \text{stage I} \quad (6)$$

$$\log \text{RDCc} = 142.1 \times (\log \sigma) - 8.36 \quad \text{stage II} \quad (7)$$

$$\log \text{RDCf} = 221.2 \times (\log \sigma) - 9.41 \quad \text{stage III} \quad (8)$$

The relationships between stress range and RDC and number of cycles to failure show the following features: At lower stress levels the number of cycles to failure increases. A similar trend, viz., with a reduction in stress level, an increase in RDC has been noticed. This could be explained in the following way: AE is produced due to microplastic strain that takes place in the material during fatigue testing. Each incremental micro plastic strain gives out an emission, irrespective of the magnitude of the strain. Hence, at low stress levels, though the magnitude of the microplastic strain is low, it is released over a larger number of cycles resulting in increased count. On the other hand, at high stress levels, the microplastic strain associated with each emission is larger but occurs in smaller number of cycles and this results in lesser number of emission counts.

Figure 6 brings out the differences in fatigue phenomena between high stress range and low stress range clearly. This figure shows the cumulative RDC versus the number of cycles for five test specimens loaded at different stress ranges. Of the five specimens, one was tested at very high range (33.8 Kg/sq.mm) and one at very low stress range (29.2 Kg/sq.mm) and the remaining three specimens between the stress ranges of 29.5 and 33.2 Kg/sq.mm. The number of cycles plotted in the figure has been normalised with respect to total number of cycles taken for fracture in each specimen. The cumulative RDC plotted on the ordinate in the same figure has also been normalised with respect to cumulative RDC recorded upto failure for each specimen. These normalised curves show different characteristics at different stress amplitude values. In general, two characteristic types were observed, one above approximately 33.8 Kg/sq.mm and one below this value. These are referred to as high stress and low stress in the present discussion.

At high stress range, deformation and microcrack formation take place in the early part of fatigue life (Hua et al.,1984). Intense acoustic emission activity is observed during this period. Further damage is gradual, indicating growth into depth and further formation of microcracks. Visual examination during these experiments did not show formation of any macro crack.

The AE activity is different in the low stress range. Damage accrues in stages with relatively quiet periods in between. The three stages of intense AE activity recorded could be related to the three stages of fatigue ascertained by metallographic studies (Tanaka,1972). It is seen that stage I takes place during early part of the fatigue life. It involves slip band formation. Stage II, which occurs almost at the middle of fatigue life marks the formation of microcracks. This stage is delineated clearly by a very large amount of AE activity. Macrocrack formation takes place at the Stage III and further damage is by the growth of the macrocrack. This part of the figure falls in line with the concept that crack initiation takes place later in fatigue life for low stress levels.

Difficulties in determining the damage in material at low stress range in early part of fatigue life are well known (Miller et al.,1981). The most interesting feature of AE is that it brings out the extent of damage that takes place until crack initiation and this can be used to ascertain damage during this period. In most of the theories on damage curve the damage is quantified only by crack length. This technique of using AE to monitor fatigue damage clearly indicates the quantum of damage on a continuous basis from the beginning to the end of fatigue life. Also in AE technique, emissions are picked up arising out of the damage not only from the surface and sub-surface but also the damage in the bulk material. The data obtained is the cumulative damage occurring throughout the material and is therefore

much more realistic than the existing methods.

DAMAGE ACCUMULATION

Though the limitations of Miner's Damage Rule are well known (Bathias et al.,1982) it continues to be employed by design engineers due to its simplicity and also due to the absence of information on the extent of damage undergone by the material on a continuous basis during fatigue testing. Acoustic Emission, which is output from the system, might describe quantitatively the extent of fatigue damage. With this in view an attempt has been made to determine fatigue damage D, by replacing the number of cycles in the numerator in the Miner's Rule by the AE parameter RDC. Hence the fatigue damage can be written as

$$D = \sum (RDC)_i / (RDC)_f \quad (9)$$

where $(RDC)_i$ is the cumulative AE count at any instant of time during testing at a stress level of σ_i ; $(RDC)_f$ is the total cumulative RDC count at failure at the same stress. The prerequisite for such a substitution is the assumption that the AE parameter, cumulative RDC count, directly reflects information concerning the non-linear nature of cumulative fatigue in a material during fatigue testing. This assumption is based on the physical nature of AE, one of whose main sources is micro-plastic strain. Therefore the failure condition in this case is the same as in equation given below when the damage, D, equals 1.

$$D = \sum (N)_i / (N)_f \quad (10)$$

Damage curves based on RDC were obtained for stress ranges varying from 29.2 Kg/sq.mm to 33.2 Kg/sq.mm by plotting an average cumulative damage curve for graphs C,D and H. Two fatigue tests were conducted, one with two step stress levels 33.2 to 29.5 Kg/sq.mm and the other with three step stress levels from 33.2 to 29.5 to 29.2 Kg/sq.mm. The actual loading schedule is given in Table 3.

Table 3 : Loading schedule to test AE Damage Curve

Sp No.	Stress/Cycle/RDC Kg/sq.mm	Stress/Cycle/RDC Kg/sq.mm	Stress/Cycle/RDC Kg/sq.mm
1-2 step	33.2/111 650 /50 000	29.5/240 480 /142 200	----
1-2-3step	33.2/20 240 /13 000	29.5/370 000 /101 000	29.2/256 300 /1 507 000

Table 4 : Damage based on Miner's Rule (number of cycles) and damage curve based on AE parameter RDC

Sp.No.	Damage based on No. of cycles.			Damage based on AE parameter RDC		
	Step I	Step II	Step III	Step I	Step II	Step III
L	0.681	0.319	--	0.769	0.237	--
M	0.124	0.491	0.305	0.2	0.135	0.55

Table 5 : Comparison of Life Prediction with actual life (for the three step loading experiment)

No. of cycles By Miner's Rule	No. of cycles By AE parameter	No. of cycles Actual
322 630	121 000	256 300

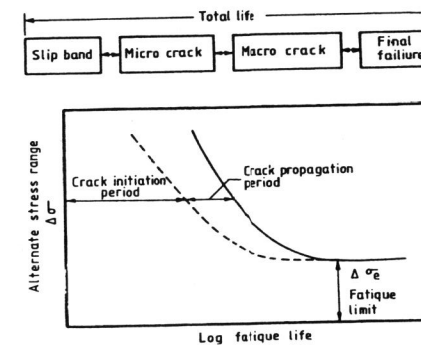


Fig. 5. Schematic of fatigue life and its dependence on stress levels (Ewalds, 1985).

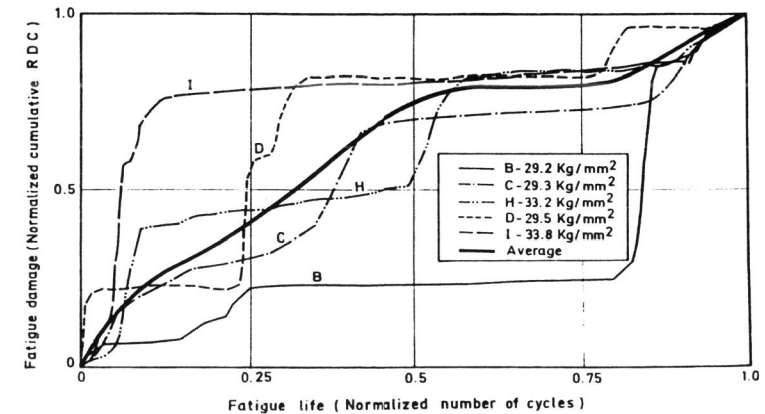


Fig. 6. Fatigue Damage curves at different stress ranges.

Table 4 shows the damage assessed based on Miner's Rule and on AE parameter RDC. The results obtained show that it is possible to assess damage based on AE parameter and this gives a more realistic indication of the damage in the material subjected to fatigue loading. The life prediction based on the AE parameter RDC is 121 000 cycles as shown in Table 5. The life prediction based on Miner's Rule is 322 630 cycles. The actual number of cycles taken by the specimen for failure is 256 300. This falls between the life prediction by AE and by Miner's Rule. However, life prediction by AE is on the conservative side. Hence, using the AE based damage curves it would be possible to predict remaining life in a component or structure.

CONCLUSIONS

1. Three active stages of fatigue damage could be determined for stress range values below 33.2 Kg/sq mm.
2. 80% of the damage occurred within 20% of fatigue life for stress levels at and above 33.8 Kg/sq.mm. Macro cracking was not observed at these stress values.
3. At stress levels less than 33.5 Kg/sq.mm extensive damage due to macro-cracking occurred during the last 20% of fatigue life as described by AE parameters.
4. The total life to failure and the fatigue stages can be related to the cumulative RDC by simple relationships.
5. The linear law of fatigue damage based on the AE output was compared with Miner's Rule, based on two-step and three-step experiments.

ACKNOWLEDGEMENT

The authors wish to thank Dr.C.R.L.Murthy, Department of Aerospace Engineering, Indian Institute of Science, Bangalore, India for providing laboratory facilities.

REFERENCES

1. Bathias, C., M. Gabra and D. Aliaga (1982). On low-cycle fatigue and life prediction. *ASTM STP 770*, pp.23-44.
2. Chaboche, J.L. (1977). A differential law of non-linear cumulative fatigue damage. Paris Institut Technique Du Batiment Et Des Travaux Publies, *HS No.39*.
3. Ewalds H.L., and R.J.H. Wanhill (1985), *Fracture Mechanics*, Co-publication of Edward Arnold, pp.170.
4. Harris D.O., D.D. Dedhia and T.C. Mamaros (1984). Acoustic emission from crack growth in steam turbine rotor steels. EPRI Research Project 734-3, Final report, pp.308.
5. Hawarth W.L., V.K. Singh and R.K. Nueller (1977). Fatigue damage detection in 2024-T3 Aluminium, Titanium and low-carbon steels by optical correlation, *J. Eng. Mat. Tech. Trans. ASME, Series H, 99*, p.319.
6. Hua C.T. and D.F. Socie (1984). Fatigue damage in 1045 steel under constant amplitude biaxial loading. *Fatigue Engng. Mater. Struct. Vol. 7, No.3*, pp. 165-179.
7. Manson S.S., J.C. Freche and C.R. Insign. Application of a double linear damage rule to cumulative fatigue. *ASTM STP 415*, pp.384-412.
8. Miller K.J. and K.P. Zachariah (1977). Cumulative damage laws for fatigue damage initiation and Stage I propagation. *J Strain Anal. 12*, pp.262-270.
9. Miller K.J. and M.F.E. Ibrahim (1981). Damage accumulation during initiation and short crack growth regimes. *Fat. of Eng. Mat. and Strct. Vol.4, No.3*, pp.263-277.
10. Miner M.A. (1945). Cumulative damage in fatigue. *J. Appl. Mech. 12*, pp. A159-A164.
11. Pangborn R.N., S. Weisman and I.R. Kramer (1981). Dislocation distribution and prediction of fatigue damage. *Met. Trans. A, Vol. 12A*, pp.109-120.
12. Tanaka, Keisuke (1972). Microscopic study of fatigue fracture strength of carbon steels, Ph D Thesis, Kyoto University.